

Algebraic charge dynamics of quantum spin-liquid β' -EtMe₃Sb[Pd(dmit)₂]₂

Shigeki Fujiyama^{1,*} and Reizo Kato¹

¹*RIKEN, Condensed Molecular Materials Laboratory, Wako 351-0198, Japan*

(Dated: 12 December 2017)

Nuclear spin-lattice ($1/T_1$) and spin-spin ($1/T_2$) relaxation rates of the cation sites of a candidate quantum spin-liquid β' -EtMe₃Sb[Pd(dmit)₂]₂ and its deuterated sample are presented. The enhanced $1/T_1$ of ¹H and ²D is thoroughly analyzed considering the rotations of methyl and ethyl groups of the cation with activation energies of 2×10^2 K and 1.2×10^3 K respectively. Contrasting charge dynamics with an algebraic temperature dependence is found at the Sb site in the EtMe₃Sb cation. The charge fluctuation remains active down to the lowest temperature, as has been observed in the ac response of dielectric constants.

I. INTRODUCTION

Quantum spin-liquids (QSLs) have attracted considerable attention in condensed matter physics.^{1,2} Geometrical frustration of the antiferromagnetic network in triangular or Kagome lattices is known to prevent classical Néel-type magnetic ordering with two sublattices and stabilize novel magnetic states. Among the QSLs, the realization of a gapless QSL whose ground state is a direct product of spin singlets, as first proposed by Anderson,³ has been pursued for a long time, however, its materialization remains a challenging issue.

Several candidate organic salts have been extensively studied.⁴ Of these, β' -EtMe₃Sb[Pd(dmit)₂]₂ (dmit = 1,3-dithiole-2-thione-4,5-dithiolate) and κ -(BEDT-TTF)₂Cu₂(CN)₃ are examined thoroughly by both magnetic and electronic measurements.⁵⁻⁸ No evidence of classical antiferromagnetic order down to $T \sim 1/1000J$ (J is the antiferromagnetic coupling constant) has been reported so far. The estimated Wilson ratio ($R_W \equiv \chi/\gamma \sim 1.1$ [emu J⁻¹K²]), which is a measure of the enhancement of the mass of quasiparticles, suggests reasonably large surfaces for the spin (spinon) excitation.⁹⁻¹¹ These experimental results are consistent with the gapless long-range resonating valence bond (RVB) scenario.

Apart from theoretical concept of the novel state, the actual material raises fundamental problems related to macroscopic quantum phenomena. One is related to the stability or robustness of the QSL against the inhomogeneity of the electronic state inherent in real materials. Although there is little opportunity for an impurity to replace the atoms in molecules in the crystallization of the organic salts, we can exemplify several sources for perturbing electronic states. For example, counter cations [in the case of Pd(dmit)₂ salts] and anions [BEDT-TTF salts] that are electronically closed shell have freedom of quenching disorders, which can cause local electronic instability. The wide distribution of the electronic spin $S = 1/2$ on [Pd(dmit)₂]₂ or (BEDT-TTF)₂ dimers also causes inhomogeneity. The tight-binding approach to compose a geometrical network of $S = 1/2$ spins cannot take the intradimer degree of freedom into account.

It was previously found that the ac responses of the dielectric constants of the molecular-based QSLs β' -

EtMe₃Sb[Pd(dmit)₂]₂ and κ -(BEDT-TTF)₂Cu₂(CN)₃ show similar anomalies.^{12,13} The dielectric constants ϵ' of both materials show enhancement between 10 K and 50 K at low frequencies below 1 MHz. The resemblance of the dielectric response for very different counter ions composed of different elements (EtMe₃Sb and Cu₂(CN)₃, both are electronically closed) indicates that the low-energy dielectric fluctuations originate from dimerized molecules that hold $S = 1/2$ spins. This is expected to disturb the geometrical network of the antiferromagnetic interaction, by which a massively degenerated ground state could be lifted. Recent theoretical works recognize the role of electric dipoles or charge fluctuations in stabilizing QSLs,¹⁴⁻¹⁶ and electronic interaction between magnetic (BEDT-TTF)₂ and anion layers is proposed as an origin for the observed ferroelectricity.^{17,18} However, the macroscopic dielectric constants cannot be compared with theoretical results, which limits quantitative understanding of the charge dynamics of QSL materials. In addition, it is known that the terminal ethylene groups in the BEDT-TTF molecule have degree of freedom in conformation, which can significantly affect the dielectric constants. Microscopic measurements of charge fluctuations have been awaited to unveil the charge dynamics of QSLs.

In this article, we report the NMR results for ¹H, ²D, and ¹²¹Sb in the cation of β' -EtMe₃Sb[Pd(dmit)₂]₂. The nuclear spin-lattice relaxation rates ($1/T_1$) and nuclear spin-spin relaxation rates ($1/T_2$) of the three elements have maxima caused by low-energy electronic fluctuations. We assign the temperature-dependent correlation times with activation energies of $\Delta = 2 \times 10^2$ and $\Delta = 1.2 \times 10^3$ to the rotations of methyl (CH₃) and ethyl (C₂H₅) groups by comparing $1/T_1$ of ¹H and ²D for pristine and d9-deuterated (C₂H₅(CD₃)₃Sb) crystals. At the Sb site, on the other hand, we found unknown glassy slowing down of the charge fluctuation with a weakly temperature-dependent correlation time, which remains active down to the lowest temperatures.

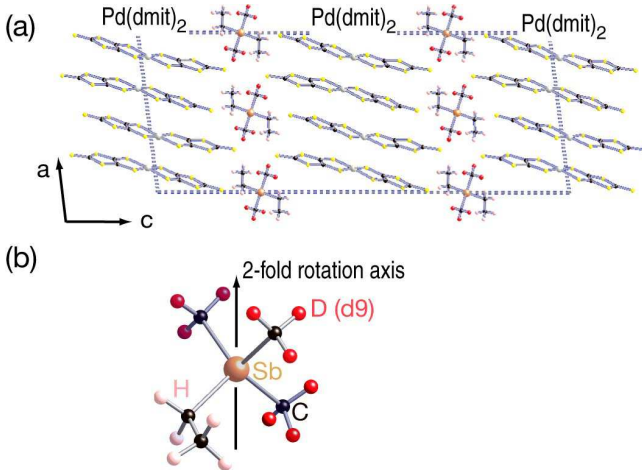


FIG. 1. (a) Crystal structure of β' -EtMe₃Sb[Pd(dmit)₂]₂. The [Pd(dmit)₂]₂ and cation layers are alternately stacked. (b) EtMe₃Sb cation. The Sb atom is located on the twofold rotation axis of the unit cell. In a d9-deuterated sample, protons of three methyl groups are labeled by deuterons.

II. EXPERIMENTALS

Single crystals of β' - X [Pd(dmit)₂]₂ ($X = \text{EtMe}_3\text{Sb}$ and Me_4Sb cations) were prepared by air oxidation of X_2 [Pd(dmit)₂] in an acetone solution containing acetic acid.¹⁹ We show in Fig. 1 the crystal structure of $X = \text{EtMe}_3\text{Sb}$. There is a twofold rotation axis of the unit cell through Sb site. NMR measurements were performed using small randomly oriented single crystals. The resonating Larmor frequencies, ω_0 , used were 125.36 MHz for ¹H, 46.5 MHz for ²D, and 79.2 MHz for ¹²¹Sb NMR. $1/T_1$ are obtained by fitting the magnetization, $M(t)$, by formulae, $M(t)/M_\infty = e^{-t/T_1}$ for ¹H, $M(t)/M_\infty = 1/4 e^{-t/T_1} + 3/4 e^{-3t/T_1}$ for ²D, and $M(t)/M_\infty = 9/35 e^{-t/T_1} + 4/15 e^{-6t/T_1} + 10/21 e^{-15t/T_1}$ for ¹²¹Sb NMR, respectively.

III. RESULTS AND DISCUSSION

We show in Fig. 2 the ²D and ¹²¹Sb NMR spectra of d9-deuterated EtMe₃Sb[Pd(dmit)₂]₂. The electric field gradient of ²D is found to be axially symmetric by Fig. 2 (a). This is consistent with the crystal structure, and we consider that the axis of the local C₃ symmetry of the CD₃ methyl group is the quantized axis of the electric field gradient of ²D. Upon lowering the temperature, the spectra show significant broadening below 40 K indicating freezing of the rotation of the methyl group. Large nuclear quadrupole moment, Q , of ¹²¹Sb compared that of ²D with $|^{121}Q|/|^{2}Q| > 10^2$ causes significant broadening of the spectra as shown in Fig. 2 (b), and no notable change is found for whole temperature. At ω_0 , the dominating source to contribute the NMR signal is the central transition, which enabled us to obtain $1/T_1$ with small

error.

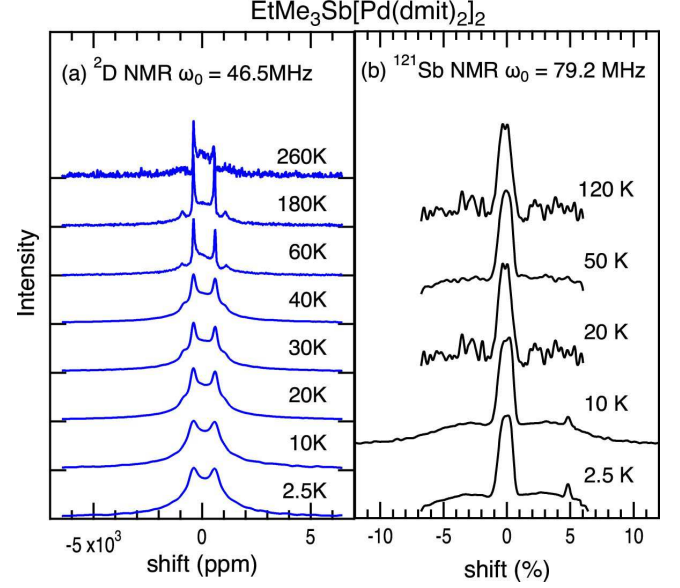


FIG. 2. NMR spectra of (a) ²D of d9-deuterated and (b) ¹²¹Sb of pristine samples of EtMe₃Sb[Pd(dmit)₂]₂. In Fig. 2 (b), ⁶³Cu signal from NMR coil is visible at $\sim 5\%$.

We plot in Fig. 3 the $1/T_1$ of ¹H, $1/T_1$ and $1/T_2$ of ¹²¹Sb for the pristine EtMe₃Sb cation, and $1/T_1$ of ¹H and ²D for the d9-deuterated cation. We also plot $1/T_1$ of ¹H for $X = \text{Me}_4\text{Sb}$, which undergoes antiferromagnetic ordering at $T_N = 11$ K, as reference data. Each data set strongly depends on the temperature, and we consider the motion in the cation as the dominant source enhancing nuclear relaxations.

In molecular solids, the rotations of methyl and ethyl groups cause magnetic and charge fluctuations of the local fields. In the case of X [Pd(dmit)₂]₂, the rotations of both groups in cation X are the sources, even though the cations are electronically closed. The fluctuation of local fields enhances $1/T_1$ as follows:²⁰

$$\frac{1}{T_1} = \langle \Delta\omega^2 \rangle \left[\frac{\tau_c}{1 + \omega_0^2 \tau_c^2} + \frac{4\tau_c}{1 + 4\omega_0^2 \tau_c^2} \right], \quad (1)$$

where $\langle \Delta\omega^2 \rangle$ is the variance of the fluctuation, which depends on the nuclear relaxation process, τ_c is the temperature dependent correlation time, and ω_0 is the Larmor frequency, which is fixed for each NMR measurement. The $1/T_1$ shows a maximum at $\omega_0 \tau_c = 0.62$.

For ¹H NMR, the relaxation is dominated by the H-H intradipolar interaction which is perturbed by rotations of methyl and ethyl groups, from which we obtain

$$\langle \Delta\omega^2 \rangle = \frac{2}{5} \left(\frac{\mu_0}{4\pi} \right) \frac{\gamma_N^4 \hbar^2}{r^6} I(I+1) \quad (2)$$

where μ_0 is the Bohr magneton, γ_N is the gyromagnetic ratio of the nuclei, r is the nearest-neighbor distance between protons, and $I = 1/2$ for ¹H.

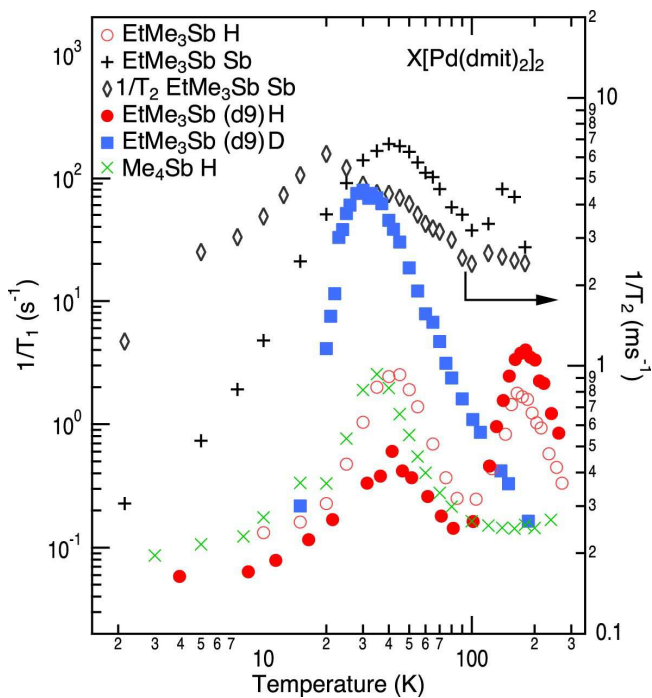


FIG. 3. Nuclear spin-lattice relaxation rates ($1/T_1$) of ^1H and ^{121}Sb for the pristine sample and those of ^1H and ^2D for the d9-deuterated sample. We plot $1/T_1$ for $X = \text{Me}_4\text{Sb}$ as reference data of a cation with tetrahedral symmetry. The black diamonds \diamond show the nuclear spin-spin relaxation rate ($1/T_2$) of Sb for the pristine sample measured at 79.2 MHz.

In the case of ^2D , which possesses a nuclear quadrupole moment, the relaxation is dominated by the fluctuation of the electric field gradient at the ^2D site and $\langle \Delta\omega^2 \rangle$ is described as^{20,21}

$$\langle \Delta\omega^2 \rangle = \frac{1}{30} \langle \omega_Q^2 \rangle, \quad (3)$$

where $\langle \omega_Q \rangle$ denotes the quadrupole coupling frequency given by

$$\omega_Q = \frac{3}{2} \frac{e^2 q Q}{\hbar}. \quad (4)$$

Here, q is the electric field gradient.

We replot the observed $1/T_1$ in Fig. 4 as well as fitted curves assuming τ_c that follows the Arrhenius equation ($1/\tau_c \propto \exp(-\Delta/T)$). The enhanced $1/T_1$ obtained by ^2D NMR for the d9-deuterated sample peaked at $1/T = 0.033 \text{ K}^{-1}$ ($T = 30\text{K}$), and comparing the corresponding suppression of $1/T_1$ of ^1H with that of the pristine sample shows that the peak at $T = 30 \text{ K}$ originated from the rotation of the methyl group, whereas that at $T = 200 \text{ K}$ is caused by the rotation of the ethyl group in the cation.

Our main interest is the temperature-dependent low-energy fluctuations of the system and the universal time constants of the electronic correlations at the three nuclear sites. We plot in Fig. 5 the correlation time τ_c of

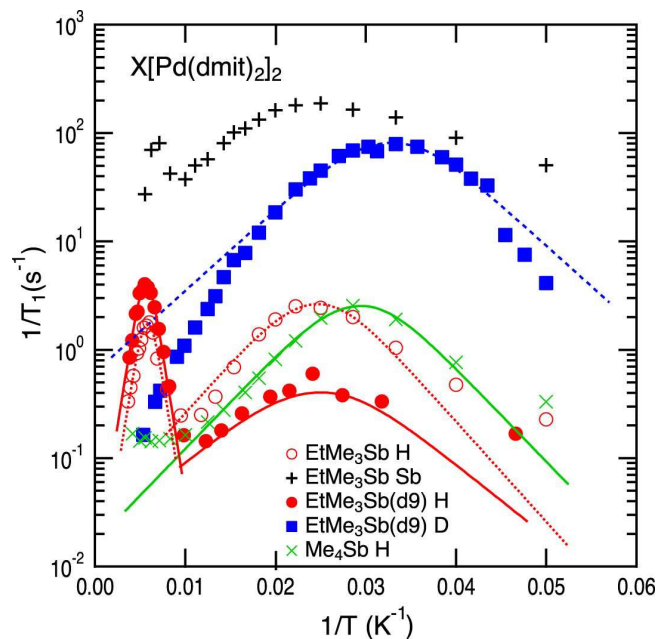


FIG. 4. Replot of $1/T_1$ shown in Fig. 3. The solid and dashed lines are fits assuming that τ_c follows the activation temperature dependence $1/\tau_c \propto \exp(-\Delta/T)$.

$1/T_1$ of ^1H , ^2D , and ^{121}Sb . $1/\tau_c$ for ^1H and ^2D almost follow the activation formula

$$1/\tau_c = 1/\tau_{c0} \exp(-\Delta/T), \quad (5)$$

where Δ is the activation energy in units of K. The solid and dashed lines in Fig. 5 are the fitted plots of $1/\tau_c$ to Eq. 5. We summarize the activation energies Δ (K) in Table I and find that Δ predominantly depends on the rotating groups and is insensitive to the nuclei observed.

The rotation of the ethyl group also enhances $1/T_1$ of Sb site peaked at $T \sim 140 \text{ K}$ as shown in Fig. 4. The obtained $1/\tau_c$ above 120 K for ^{121}Sb well agrees that for ^1H as shown in Fig. 5. This indirect effect to the local fluctuation of the electric field gradient at Sb site indicates that the rotation axis of the ethyl group is a skew line to the Sb-C bonds, by which local field is perturbed.

Below 100 K, however, $1/\tau_c$ for ^{121}Sb has no characteristic activation energy but slows down gradually, which crosses $1/\tau_c$ for ^2D and ^1H originating from the methyl rotation. This shows little indirect coupling between the electric field gradient at the Sb site and the rotation of the methyl group, which is consistent with the ^2D NMR spectra with axial symmetry. The rotation axis agrees to the Sb- CH_3 bonds and the local rotation is not seriously perturb the electronic state at Sb. This argument is supported by contrasting magnitudes of the enhancements of $1/^{121}\text{T}_1$ for two peaks, while nearly the same enhancements of $1/^{1}\text{T}_1$ are observed for the rotations of the ethyl and methyl groups. $1/\tau_c$ is fitted by a power relation to the temperature as $1/\tau_c \propto T^\nu$ with $\nu = 2.5$. This glassy slowing down of $1/\tau_c$ well explains the peak of $1/T_2$ at 20 K shown in Fig. 3 because the energy of $1/T_2$

TABLE I. Activation energies Δ of the correlation time τ_c of the rotations of methyl and ethyl groups of the pristine and d9-deuterated $X=\text{EtMe}_3\text{Sb}$ and $X=\text{Me}_4\text{Sb}$ of $X[\text{Pd}(\text{dmit})_2]_2$. The rotation axis of the ethyl of d9-deuterated sample does not agree to the Sb-C bonds, which cause a small enhancement of $1/T_1$ for ^1H in the ethyl group by indirect coupling. The unit is K.

	pristine sample		d9-deuterated		Me ₄ Sb
	H		H	D	H
Methyl	213		(153)	172	198
Ethyl	1175		1206	-	-

is characterized by the dephasing process of the nuclear magnetizations at ~ 100 kHz.²²

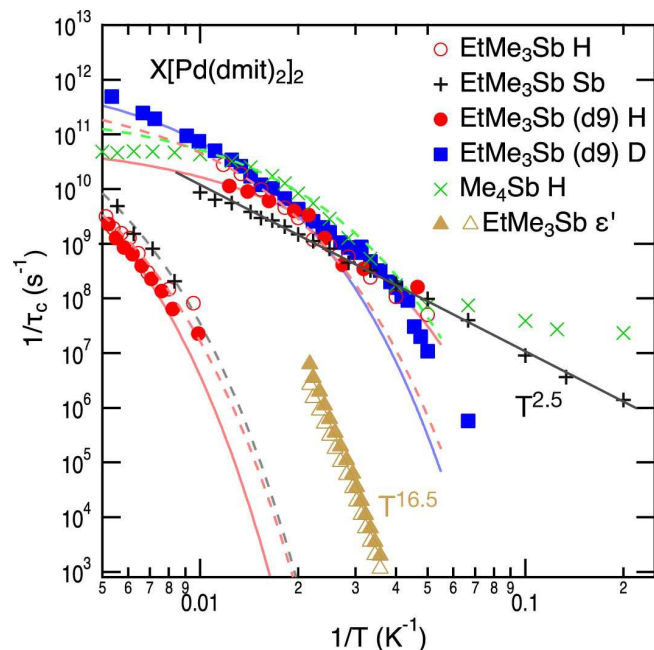


FIG. 5. Temperature-dependent correlation time τ_c of the cation sites of $X[\text{Pd}(\text{dmit})_2]_2$ obtained by fitting the data by Eq. 1. The peak temperature of the dielectric constant as a function of the oscillating frequency (unit of radian) is shown as closed triangles.¹³ Corrected microscopic time constants τ_m of the dielectric constants are shown as open triangles. Solid and dashed curves follow the activation temperature dependence. $1/\tau_c$ for ^{121}Sb NMR and the dielectric constant appear linear in the plot and follow an algebraic temperature dependence.

The nuclear relaxations of the proton and deuteron NMR unveil the rotations of methyl and ethyl groups, whose temperature dependence follows Eq. 1. For β' - $\text{EtMe}_3\text{Sb}[\text{Pd}(\text{dmit})_2]_2$, a similar enhanced dielectric constant was reported in Ref. 13. Although the enhancement of the dielectric response shows the slow charge dynamics of the sample, it is still under debate whether the magnetically active $[\text{Pd}(\text{dmit})_2]_2$ dimers or the cations that is electronically closed cause the slow fluctuation of the

electrons.

The dielectric response at the classical limit is expressed as

$$\epsilon(\omega) = \epsilon_\infty + \frac{\epsilon_0 - \epsilon_\infty}{i\omega\tau_M} \quad (6)$$

Here, ϵ_∞ and ϵ_0 denote the dielectric constants at the highest- and lowest-frequency limits, τ_M is the characteristic time constant for macroscopic polarization, respectively.

Equation 6 is expected to have a maximum at $\omega\tau_M = 1$. We plot in Fig. 5 the inverted oscillating frequency (unit is $\text{rad} [\text{s}^{-1}]$) as a function of the peak temperature of the dielectric constant. $1/\tau_M$ for the dielectric constant lies between the two values of $1/\tau_c$ for the rotations of the ethyl and methyl groups. $1/\tau_M$ is $\sim 10^5$ times smaller than $1/\tau_c$ for the rotation of the ethyl group and $\sim 10^5$ times larger than $1/\tau_c$ of that of the methyl group of the cation. The temperature dependence of $1/\tau_M$ follows an algebraic relation with temperature, $1/\tau_c \propto T^\nu$ with $\nu = 16.5$, while the two values of $1/\tau_c$ follow the activation temperature dependence. The contrasting values and temperature dependences of τ_M and τ_c show that the electronic fluctuations by the rotations of the methyl and ethyl groups do not directly cause the enhancement of the dielectric constant. We examine the relation between τ_M and microscopic relaxation time τ_m of dipole moments, which should be more favorable for comparison with τ_c measured by NMR. We apply the widely accepted formula $\tau_M = 3\epsilon_0\tau_m/(2\epsilon_0 - \epsilon_\infty)$ ^{23,24} and plot τ_m using the values of $\epsilon(\omega)$ at 1 MHz and 316 Hz for ϵ_∞ and ϵ_0 , respectively. This correction is not ideal, but the correction factor $3\epsilon_{316\text{Hz}}/(2\epsilon_{316\text{Hz}} - \epsilon_{1\text{MHz}})$ shows a moderate change on the order of unity, ranging from 1.7 at 28 K to 2.3 at 46 K. We plot τ_m in Fig. 5 as open triangles and find that the correction has a minor effect on the estimated correlation time.

Whereas the motion of the methyl and ethyl groups has little impact on the dielectric response, we can claim a correspondence between the slow charge dynamics and the fluctuation of the local electric field at the Sb site of the EtMe_3Sb cation. $1/\tau_c$ for ^{121}Sb NMR shows an unconventional slowing down of the local field following the power relation $1/\tau_c \propto T^\nu$ with $\nu = 2.5$. Although the two indices ν for the dielectric constant and the local fluctuation of the electric field are different, both electric responses exhibit glassy slowing down of multiple electric potentials. This argument again supports the conclusion in Ref. 13 that applied a Fourier-transformed stretched exponential function to analyze $\epsilon'(\omega)$. Shift from the simplest Debye formula shows a glassy electronic state.

The observed algebraic electric fluctuations have the potential to promote the emergence of a QSL. The correlation time of the fluctuation at ^{121}Sb continues to survive $1/\tau_c > 10^6 \text{ s}^{-1}$, even at $T = 5$ K, which can disturb classical magnetic ordering. The power relations of the correlation times to the temperature $1/\tau_{c,M} \propto T^\nu$ observed by NMR and the dielectric constants have no fi-

nite critical temperature, suggesting the existence of the quantum critical point at zero temperature. In addition, it has been theoretically well established that quantum liquids in one and two dimensions are characterized by algebraic electronic correlations, and our results are in line with this understanding.^{25,26} While the origin of the observed glassy state is still open, we comment that nearly degenerate energy levels in a QSL are on the verge of algebraic particle excitations and a concomitant glassy state in space and time domains.

IV. SUMMARY

In this report, we demonstrated the nuclear spin-lattice and spin-spin relaxations of the cation of the candidate quantum spin-liquid β' -EtMe₃Sb[Pd(dmit)₂]₂. Significant enhancements of $1/T_1$ and $1/T_2$ were observed at ¹H and ¹²¹Sb in the pristine sample and at ¹H, ²D in the d9-deuterated samples. The correlation times follow the

activation temperature dependence, and we estimate the activation energies $\Delta = 2 \times 10^2$ K (1.2×10^3 K) for the rotation of the methyl (ethyl) group respectively.

An unconventional charge dynamics was found for the Sb site in the cation. The algebraic slowing down of the charge dynamics with a small exponent, $1/\tau_c \propto T^{2.5}$, shows that the charge fluctuation remains active even at the lowest temperature, which can prevent classical magnetic ordering and stabilize QSL. The observation of the algebraic charge dynamics shows that charge correlation as well as magnetic correlation can be strongly modified in quantum liquids.

ACKNOWLEDGMENTS

We are grateful to K. Ueda for helpful discussions. This work was supported by Grants-in-Aid for Scientific Research (C) (26400378) and (S) (16H06346) from JSPS.

-
- * E-mail: fujiyama@riken.jp
- ¹ L. Balents, *Nature* **464**, 199 (2010).
 - ² L. Balents, M. P. A. Fisher, and S. M. Girvin, *Phys. Rev. B* **65**, 224412 (2002).
 - ³ P. W. Anderson, *Materials Research Bulletin* **8**, 153 (1973).
 - ⁴ K. Kanoda and R. Kato, *Annual Review of Condensed Matter Physics* **2**, 167 (2011).
 - ⁵ M. Tamura and R. Kato, *Journal of Physics: Condensed Matter* **14**, L729 (2002).
 - ⁶ Y. Shimizu, K. Miyagawa, K. Kanoda, M. Maesato, and G. Saito, *Phys. Rev. Lett.* **91**, 107001 (2003).
 - ⁷ Y. Kurosaki, Y. Shimizu, K. Miyagawa, K. Kanoda, and G. Saito, *Phys. Rev. Lett.* **95**, 177001 (2005).
 - ⁸ Y. Shimizu, T. Hiramatsu, M. Maesato, A. Otsuka, H. Yamochi, A. Ono, M. Itoh, M. Yoshida, M. Takigawa, Y. Yoshida, and G. Saito, *Phys. Rev. Lett.* **117**, 107203 (2016).
 - ⁹ M. Yamashita, N. Nakata, Y. Senshu, M. Nagata, H. M. Yamamoto, R. Kato, T. Shibauchi, and Y. Matsuda, *Science* **328**, 1246 (2010).
 - ¹⁰ S. Yamashita, Y. Nakazawa, M. Oguni, Y. Oshima, H. Nojiri, Y. Shimizu, K. Miyagawa, and K. Kanoda, *Nat Phys* **4**, 459 (2008).
 - ¹¹ S. Yamashita, T. Yamamoto, Y. Nakazawa, M. Tamura, and R. Kato, *Nature Communications* **2**, 275 EP (2011).
 - ¹² M. Abdel-Jawad, I. Terasaki, T. Sasaki, N. Yoneyama, N. Kobayashi, Y. Uesu, and C. Hotta, *Phys. Rev. B* **82**, 125119 (2010).
 - ¹³ M. Abdel-Jawad, N. Tajima, R. Kato, and I. Terasaki, *Phys. Rev. B* **88**, 075139 (2013).
 - ¹⁴ C. Hotta, *Phys. Rev. B* **82**, 241104 (2010).
 - ¹⁵ M. Naka and S. Ishihara, *Journal of the Physical Society of Japan* **79**, 063707 (2010).
 - ¹⁶ M. Naka and S. Ishihara, *Journal of the Physical Society of Japan* **84**, 023703 (2015).
 - ¹⁷ M. Dressel, P. Lazić, A. Pustogow, E. Zhukova, B. Gorshunov, J. A. Schlueter, O. Milat, B. Gumhalter, and S. Tomić, *Phys. Rev. B* **93**, 081201 (2016).
 - ¹⁸ M. Pinterić, P. Lazić, A. Pustogow, T. Ivek, M. Kuveždić, O. Milat, B. Gumhalter, M. Basletić, M. Čulo, B. Korinhamzić, A. Löhle, R. Hübner, M. Sanz Alonso, T. Hiramatsu, Y. Yoshida, G. Saito, M. Dressel, and S. Tomić, *Phys. Rev. B* **94**, 161105 (2016).
 - ¹⁹ R. Kato and C. Hengbo, *Crystals* **2**, 861 (2012).
 - ²⁰ C. Dimitropoulos, J. Pelzl, and F. Borsa, *Phys. Rev. B* **41**, 3914 (1990).
 - ²¹ A. Abragam, *The Principles of Nuclear Magnetism*, International series of monographs on physics (Clarendon Press, 1961).
 - ²² S. Fujiyama, M. Takigawa, and S. Horii, *Phys. Rev. Lett.* **90**, 147004 (2003).
 - ²³ J. G. Powles, *The Journal of Chemical Physics* **21**, 633 (1953).
 - ²⁴ R. H. Cole, *The Journal of Chemical Physics* **42**, 637 (1965).
 - ²⁵ H. C. Po and Q. Zhou, *Nature Communications* **6**, 8012 (2015).
 - ²⁶ F. D. M. Haldane, *Journal of Physics C: Solid State Physics* **14**, 2585 (1981).